Light-Induced Proton Release and Proton Uptake Reactions in the Cyanobacterial Phytochrome Cph1[†]

Jasper J. van Thor,*[,‡,§] Berthold Borucki,[§,||] Wim Crielaard,[‡] Harald Otto,[||] Tilman Lamparter,[⊥] Jon Hughes,[⊥,#] Klaas J. Hellingwerf,[‡] and Maarten P. Heyn[||]

Laboratory for Microbiology, Swammerdam Institute for Life Sciences, University of Amsterdam, Nieuwe Achtergracht 166, 1018 WV Amsterdam, The Netherlands, Biophysics Group, Department of Physics, Freie Universität Berlin, Arnimallee 14, D-14195 Berlin, Germany, and Plant Physiology, Freie Universität Berlin, Königin-Luise-Strasse 12-16, D-14195 Berlin, Germany

Received November 17, 2000; Revised Manuscript Received June 7, 2001

ABSTRACT: The P_r to P_{fr} transition of recombinant *Synechocystis* PCC 6803 phytochrome Cph1 and its N-terminal sensor domain Cph1Δ2 is accompanied by net acidification in unbuffered solution. The extent of this net photoreversible proton release was measured with a conventional pH electrode and increased from less than 0.1 proton released per P_{fr} formed at pH 9 to between 0.6 (Cph1) and 1.1 (Cph1Δ2) H^+/P_{fr} at pH 6. The kinetics of the proton release were monitored at pH 7 and pH 8 using flash-induced transient absorption measurements with the pH indicator dye fluorescein. Proton release occurs with time constants of ∼4 and ∼20 ms that were also observed in parallel measurements of the photocycle (τ_3 and τ_4). The number of transiently released protons per P_{fr} formed is about one. This H^+ release phase is followed by a proton uptake phase of a smaller amplitude that has a time constant of ∼270 ms (τ_5) and is synchronous with the formation of P_{fr}. The acidification observed in the P_r to P_{fr} transition with pH electrodes is the net effect of these two sequential protonation changes. Flash-induced transient absorption measurements were carried out with Cph1 and Cph1Δ2 at pH 7 and pH 8. Global analysis indicated the presence of five kinetic components ($\tau_1-\tau_5$: 5 and 300 μs and 3, 30, and 300 ms). Whereas the time constants were approximately pH independent, the corresponding amplitude spectra (B_1, B_3, and B_5) showed significant pH dependence. Measurements of the P_r/P_{fr} photoequilibrium indicated that it is pH independent in the range of 6.5−9.0. Analysis of the pH dependence of the absorption spectra from 6.5 to 9.0 suggested that the phycocyanobilin chromophore deprotonates at alkaline pH in both P_r and P_{fr} with an approximate pK_a of 9.5. The protonation state of the chromophore at neutral pH is therefore the same in both P_r and P_{fr}. The light-induced deprotonation and reprotonation of Cph1 at neutral pH are thus due to pK_a changes in the protein moiety, which are linked to conformational transitions occurring around 4 and 270 ms after photoexcitation. These transient structural changes may be relevant for signal transduction by this cyanobacterial phytochrome.

Phytochromes were found and characterized initially in higher plants, where they regulate numerous developmental processes such as germination, synthesis of the photosynthetic apparatus, hypocotyl elongation, shade avoidance, and flowering (for review, see refs *1* and *2*). From the *Synechocystis* PCC 6803 genome sequencing project, a phytochrome-like gene *slr0473* was identified (*3*) and after heterologous expression in *Escherichia coli* yielded apophytochrome that autoassembled with linear tetrapyrrole chromophores to produce spectrally active holophytochrome Cph1 (*4*−*6*).[1] This is a light-regulated histidine kinase of the two-component type (*6*, *7*). Cph1 has a lower molecular mass than plant phytochromes (85 vs 124 kDa), lacking the 300-residue PAS module that is important for signal transduction in plant phytochromes (*7*).

For plant phytochromes, phototransformation from P_r to P_{fr} is known to involve a (*Z*,*E*) photoisomerization around the 15,16-double bond connecting the C- and D-ring of the linear tetrapyrrole (for a review, see ref *8*). Plant phyto-

[†] This work was supported by grants from the Deutsche Forschungsgemeinschaft to T.L. (Sfb 498, TP B2), J.H. (Sfb 498, TP B2), and M.P.H. (Sfb 498, TP B1).

* To whom correspondence should be addressed. Present address: University of Oxford, Laboratory of Molecular Biophysics, Rex Richards Building, South Parks Road, Oxford OX1 3QU, U.K. Phone: +44-(0)1865-275374; fax: +44-(0)1865-275182; e-mail: jasper@biop.ox.ac.uk.

[‡] University of Amsterdam.

[§] These authors contributed equally to this work.

[||] Department of Physics, Freie Universität Berlin.

[⊥] Plant Physiology, Freie Universität Berlin.

[#] Present address: Plant Physiology, University of Giessen, D-35392 Giessen, Germany.

[1] Abbreviations: Cph1, cyanobacterial phytochrome 1; Cph1Δ2, N-terminal chromophore carrying domain of Cph1 lacking the histidine kinase domain; P_r, red light absorbing state; P_{fr}, far-red light absorbing state; PCB, phycocyanobilin; fwhm, full width at half-maximum; Q_y-band, long-wavelength absorption band of phytochrome; LED, light-emitting diode; SVD, singular value decomposition; PAS, acronym formed from the names of the first three proteins (period clock protein of *Drosophila*, aryl hydrocarbon receptor nuclear translocator of vertebrates, single-minded protein of *Drosophila*) recognized as sharing this sensory domain. mOD: milli.OD.

10.1021/bi002651d CCC: $20.00
Published on Web 08/29/2001

chromes carry the linear tetrapyrrole chromophore phytochromobilin (PΦB), which differs from phycocyanobilin (PCB), the dominant bilin in *Synechocystis* PCC 6803, by a single bond terminal to ring D. It has recently been shown that affinity-tagged Cph1, purified from *Synechocystis*, contains PCB as its chromophore (*9*). In this study, we investigated recombinant Cph1 assembled with PCB.

Phototransformation properties of recombinant Cph1 have been studied with respect to their kinetic and spectral characteristics during the $P_r \rightarrow P_{fr}$ transition by flash-photolysis measurements and with FT resonance Raman spectroscopy of the ground states P_r and P_{fr} (*10*). This has revealed basic similarities between Cph1 and higher plant phytochromes, such as PhyA from oat. Among the differences is the occurrence of an intermediate with a rise time of ~300 μs and a decay time of ~3 ms that is absent in PhyA (*10*). The rise and decay kinetics of this intermediate display a strong deuterium isotope effect, suggesting that these transitions are associated with rate-limiting proton-transfer steps (*10*). Recently, UV/vis and FTIR measurements of recombinant Cph1 have shown that photocycle intermediates, trapped at low temperature, can be assigned to the meta-R_a and meta-R_c states in the $P_r \rightarrow P_{fr}$ pathway and to lumi-F and meta-F in the $P_{fr} \rightarrow P_r$ pathway (*11*).

Phytochromes are members of the large family of photoreceptor proteins. In other members of this family, such as the mammalian rhodopsins (*12*−*14*), sensory rhodopsins (e.g., see ref *15*), and photoactive yellow proteins (*16*, *17*), intramolecular proton transfer between the chromophore and the protein moiety as well as transient release and uptake of protons from the aqueous medium play important roles in the mechanism of their activation and in the formation of the signaling state. In the case of the light-driven proton pump bacteriorhodopsin, these two proton-transfer processes are also directly linked: the deprotonation of the chromophore is kinetically coupled to the release of a proton to the external medium by a residue at the extracellular surface (*18*). Whether similar proton-transfer reactions are occurring in the cyanobacterial phytochrome Cph1 is currently unknown. It was thus the aim of the present paper to investigate possible light-induced protonation changes of the protein moiety and of the chromophore of Cph1. Net and transient release and uptake of protons from the aqueous medium were monitored using pH electrodes and optical pH indicator dyes. The deprotonation of the chromophore in P_r and P_{fr} was investigated by measuring the pH dependence of the absorption spectra of these two species and of the P_r/P_{fr} photoequilibrium.

The chemical basis of this change in protonation state can range from p*K* shifts associated with the formation of transient states of their chromophore to uptake or release of protons due to p*K* changes associated with conformational transitions. The latter process is widespread in biochemistry and was first studied in detail for hemoglobin (*19*). The protons that are released or taken up due to conformationally induced p*K* changes are often referred to as Bohr protons (*19*).

For pea phytochrome A, steady-state measurements using pH electrodes have demonstrated a photoreversible change in protonation in the P_r to P_{fr} transition (*20*−*22*). Depending on the pH, either an alkalinization (net proton uptake, at low pH) or an acidification (net proton release, at high pH) of the medium was observed with the 114-kDa fragment. For the native 121-kDa phytochrome, on the other hand, almost no net proton release or uptake was observed at any pH, suggesting that a N-terminal segment prevents net proton transfer to the medium (*21*). Complementary steady-state resonance Raman measurements indicated that the chromophore was protonated in P_r but deprotonated in the I_{bl} intermediate and in P_{fr} (*23*). Together with the results from the pH-electrode measurements, this led to the interpretation that in native pea phytochrome the chromophore deprotonates between the I_{700} and the I_{bl} intermediates, causing the transient release of a proton to the external medium (*23*). In the transition between I_{bl} and P_{fr}, a proton is taken up again by an amino acid side chain of the protein moiety (*23*). No direct temporal evidence was provided for this sequence of proton release and uptake events. Moreover, there is strong evidence from resonance Raman and FTIR experiments that the tetrapyrrole chromophore of PhyA phytochrome from plants is protonated in P_r, P_{fr}, and all its intermediates (*24*−*26*). The same conclusion was recently reached for the P_r, P_{fr}, and meta-R_a states of Cph1 (*11*). Because of a lack of studies with isotopically substituted chromophores, the band assignments to particular vibrations are not yet certain however. The interpretation of ref *23* therefore cannot be ruled out at present.

The Cph1 phytochrome from *Synechocystis* differs from plant phytochromes in at least three important aspects: it lacks the plant phytochrome PAS module, the P_r form shows the histidine kinase activity, and it has a strong kinetic isotope effect associated with a novel intermediate that is unique to Cph1 (*10*). It is thus of major interest to investigate whether this prokaryotic phytochrome also changes its protonation state in the P_r to P_{fr} photoconversion. Moreover, to make progress in understanding the functional significance and mechanism of these proton transfer reactions, it is clearly essential to be able to associate these steps with particular transitions between transient intermediates on the pathway between P_r and P_{fr}.

Here, we present the results of investigations on the protonation states of both the protein and the cofactor moieties in P_r and P_{fr} and on the light-induced transient proton release and uptake reactions in recombinant cyanobacterial phytochrome. These experiments were carried out with the full-length Cph1 (85 kDa) as well as the N-terminal chromophore-carrying domain Cph1Δ2 (58 kDa) that lacks the C-terminal transmitter domain. In both systems, the apoprotein was assembled with PCB as the chromophore. Complementary measurements of the pH dependencies of the phytocycles and of the P_r/P_{fr} photoequilibrium were undertaken to allow a comprehensive interpretation of the protonation experiments. We found that over the entire accessible pH range from 5.5 to 9.5 the P_r to P_{fr} transition is accompanied by net proton release (acidification). Time-resolved measurements of the proton concentration showed that this is the net result of a phase of transient proton release associated with the decay of a 3-ms intermediate followed by a phase of transient proton uptake of smaller amplitude that is associated with the formation of P_{fr} (270 ms). At pH 7, the chromophore is probably protonated in both P_r and P_{fr}. The sources of the protons are thus most likely the ionizable amino acid side chains of the protein moiety that experience light-induced p*K* changes associated with transient

and permanent structural changes between P_r, P_{fr}, and the 3-ms intermediate.

MATERIALS AND METHODS

Sample Preparation. Recombinant *Synechocystis* PCC6803 Cph1 (85 kDa) as well as a 58-kDa truncated fragment of Cph1Δ2, lacking the C-terminal histidine kinase domain (*6*), were expressed with C-terminal $(His)_6$ tags in *E. coli*, purified on Ni^{2+}−NTA (Qiagen), and auto-assembled with PCB as described previously (*4*, *5*). Medium exchange and buffer removal were performed immediately prior to the pH measurements by size-exclusion chromatography on Sephadex G-50 fine (Pharmacia).

Simultaneous Transient pH and UV/Vis Absorption Measurements. Unbuffered samples of Cph1 and Cph1Δ2 were used at a concentration of ∼20 μM (OD_{660} ∼ 1.5; optical path length, 1 cm) in 1 M KCl. Simultaneous measurement of the pH and absorption spectra was performed as described earlier (*17*), using a "Kraayenhof vessel" (*27*), a cuvette equipped with both an adapter for illumination and a pH electrode (Mettler-Toledo, InLab 423). For pH measurements, four far-red light-emitting diodes (LEDs) were used for more efficient excitation of P_{fr}, resulting in faster electrode measurements (Figure 1A). pH was adjusted with small aliquots of 0.01 M KOH or HCl, and the extent of the pH change was calibrated by the addition of microliter aliquots of 2.5 mM oxalic acid ($pK_{a(1)} = 1.23$; $pK_{a(2)} = 4.19$). Temperature was maintained at 20 °C.

Spectroscopy. Time-resolved (second time scale) UV/vis absorption spectra were recorded with a Hewlett-Packard diode array spectrophotometer model HP 8453 (Portland, OR). Phototransformation measurements were performed with the Kraayenhof vessel in place (*27*). The sample was stirred and illuminated in a 90° geometry with either a far-red LED (λ_{em} = 735 nm, 28 nm fwhm, Quantum Devices, P/N QDDH73502, operated at 20 mA, 4.06 mW) or a red LED (λ_{em} = 644 nm, 37 nm fwhm, HP-HLMP4100, operated at 20 mA, 0.27 mW). Steady-state absorption spectra with a resolution of 0.45 nm were recorded with an Aminco DW2000 UV/vis spectrophotometer (SLM Instruments Inc., Urbana, IL), calibrated with a holmium filter. Here, the pH was adjusted by adding small volumes of concentrated Tris-HCl buffer to unbuffered phytochrome solutions. The optical path length was 1 cm in the time-resolved and the steady-state measurements.

Phototransformation rates were analyzed essentially according to the Butler's initial rate method (*28*, *29*) but accounting for the nonmonochromatic emission of the LEDs according to

$$\frac{\phi_R}{\phi_{FR}} = \frac{I_{(LED735)}\int L_{(LED735)}(\nu)A_{eq}^{644}(\nu)\,d\nu\,(dA_{720}/dt)^{644}}{I_{(LED644)}\int L_{(LED644)}(\nu)A_{eq}^{735}(\nu)\,d\nu\,(dA_{720}/dt)^{735}} \quad (1)$$

and

$$1 - x_{P_{fr}}^{644} = \frac{1}{1 + \dfrac{\phi_R}{\phi_{FR}}} \frac{\int L_{(LED644)}(\nu)A_{eq}^{644}(\nu)\,d\nu}{\int L_{(LED644)}(\nu)A_{eq}^{735}(\nu)\,d\nu} \quad (2)$$

where ϕ_R and ϕ_{FR} are the quantum yields for the $P_r \rightarrow P_{fr}$ and $P_{fr} \rightarrow P_r$ transitions, respectively; $I_{(LED735)}$ and $I_{(LED644)}$ are the intensities of the 735- and the 644-nm LEDs; $L_{(LED735)}(\nu)$ and $L_{(LED644)}(\nu)$ are the energy-normalized emission spectra of the 735- and 644-nm LEDs; $A_{eq}^{644}(\nu)$ and $A_{eq}^{735}(\nu)$ are the absorption spectra of Cph1 in photoequilibrium with 644- and 735-nm light; $x_{P_{fr}}^{644}$ is the mole fraction of P_{fr} present in photoequilibrium with 644-nm excitation; $(dA_{720}/dt)^{644}$ is the initial rate of absorption change at 720 nm when the far-red irradiated solution (i.e., pure P_r) is excited at 644 nm; and $(dA_{720}/dt)^{735}$ is the initial rate of absorption change at 720 nm when the red irradiated solution (P_r/P_{fr} equilibrium) is excited at 735 nm.

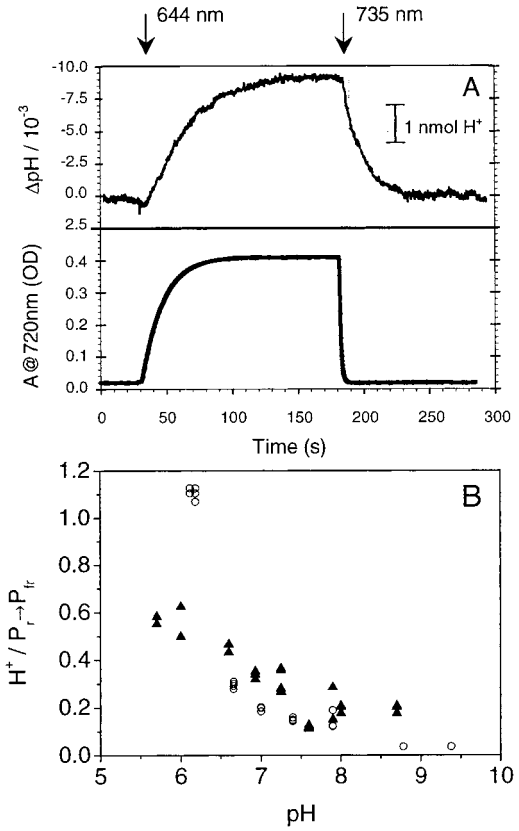

FIGURE 1: Simultaneous recording of light-induced acidification and absorption changes. Unbuffered samples of Cph1 and Cph1Δ2 (in 1 M KCl, 20 °C) were irradiated with either red (644 nm) or far-red light (735 nm) with continuous monitoring of the pH. (A) Example of pH-electrode recording and simultaneous recording of absorption changes at 720 nm, reflecting P_{fr} formation, of Cph1Δ2 at pH 7.0. The bar represents the size of the pH change upon addition of 1 nmol of H^+ (volume: 1.8 mL). The delay of the pH-electrode transients relative to the kinetics of P_r and P_{fr} formation is due to the mixing time of the setup and the response time of the electrode. (B) Plot of the $H^+/P_r \rightarrow P_{fr}$ stoichiometry measured for Cph1 (▲) and Cph1Δ2 (○) as a function of pH. The electrode recording was calibrated at each pH value using microshots of oxalic acid.

Transient Absorption Spectroscopy. Laser flash-induced absorption traces were recorded using a laboratory-built flash-photolysis apparatus with an output power of about 2 mJ at 640 nm (10-ns pulse length) (*30*). This instrument has a logarithmic time base, allowing transient absorption changes to be measured from the nanosecond to the second time domain. For excitation in the long wavelength absorption band of P_r, the laser dye 4-(dicyanomethylene)-2-methyl-6-(4-dimethylaminostyryl)-4*H*-pyran (DCM) was used, dissolved at a concentration of 0.7 g/L in propylene carbonate.

Two methods were used to ensure that before each flash excitation the P_r form was fully reformed. In the first method, continuous far-red light was applied from a 150-W lamp (KL 1500, Schott) filtered through a 715-nm high-pass filter (RG9). In the second method, the sample was preilluminated by the same light source for 15 s before the excitation flash, thereby fully reforming P_r. In these two methods, the time intervals between subsequent measurements were 24 and 6 s, respectively. The most complete sets of data, allowing calculation of amplitude spectra, were collected at 22 or 27 wavelengths between 545 and 755 nm. For many purposes, kinetic traces at 655, 675, and 705 nm were sufficient. The bandwidth was 8 nm. At each wavelength, 20−30 transients were averaged. The temperature was maintained at 22 °C.

Samples of Cph1 and Cph1Δ2 were prepared at an $OD_{660} \sim 1.5$ (optical path length, 1 cm) in 50 mM KCl (pH 7.0−8.5), degassed, and flushed with nitrogen. Sodium−fluorescein (Molecular Probes; relevant $pK_a = 6.4$) was added to samples at 13 μM concentration ($OD_{490} = 0.7$ at pH 7.0). Proton release and proton uptake kinetics were recorded by measuring the absorption changes at 490 nm (absorption maximum of deprotonated fluorescein) of unbuffered samples with and without indicator. The difference between these two traces reflects the transient proton signal (*31*). Fluorescein was selected as the pH indicator dye since at its λ_{max} (490 nm) the transient absorption changes of Cph1 are minimal. Proton release was calibrated using an oxalic acid microtitration.

Singular-value decomposition (SVD) calculations were performed with Mathematica 3.0. For simultaneous fitting of the time traces, Origin 5.0 software was used.

RESULTS

Light-Induced Reversible Acidification of Unbuffered Solutions of Phytochrome. Recent experiments on PYP (*16*, *17*, *32*), green fluorescent protein (*33*, *34*), and rhodopsin (*35*, *36*) have shown that measurement of protonation processes can uncover crucial details about the conformational transitions that follow light absorption by these photoactive proteins. To investigate whether similar processes play a role in the photoactivation of the bacterial phytochrome Cph1, we analyzed the pH changes that occur upon illumination in unbuffered suspensions of Cph1 and Cph1Δ2, its C-terminally truncated variant. To obtain a stable reading from the pH electrode, a salt concentration of 1 M KCl was necessary (*17*, *37*). Figure 1A shows typical results obtained from simultaneous recording of the pH (upper panel) and absorbance (lower panel) changes of a solution containing Cph1Δ2. Starting in the P_r state, partial conversion to P_{fr} by red light of 644 nm leads at pH 7 to stable acidification, i.e., net proton release. As shown in Figure 1A, the acidification was fully reversed by illumination with far-red light of 735 nm. Similar observations were made with Cph1. After calibration of the pH changes with oxalic acid microtitration between pH 5.5 and pH 9.5, the measurement of the light-induced absorption changes allowed calculation of the $H^+/P_r \rightarrow P_{fr}$ stoichiometry. In this calculation, the difference in extinction between P_r and P_{fr} at the specific pH values was taken into account (see below, Figure 2A,B). Figure 1B shows that the extent of the photoreversible acidification in P_{fr} increased with decreasing pH values for both Cph1 (▲) and Cph1Δ2 (○).

Dependence of P_r and P_{fr} Spectra on pH, Phototransformation Rates, and Quantum Yield Ratios. To study the protonation state of the chromophore and the protein moiety in P_r and P_{fr}, spectral and kinetic data in the second time domain were collected during phototransformation reactions at different pH values. Spectral and kinetic data were collected for the $P_r \rightarrow P_{fr}$ and the $P_{fr} \rightarrow P_r$ transition. Spectra were taken after saturating illumination with 644-nm light (which establishes a photoequilibrium between P_r and P_{fr}, requiring ca. 300 s at the given light intensity) and 735-nm light (which fully depletes P_{fr}), respectively. Time traces were recorded at 720 nm (while illuminating with 644-nm light, starting from the pure P_r state) and under illumination with 735-nm light (starting from the P_r-P_{fr} photoequilibrium described above). From these two time traces, the initial rates of absorbance change were determined. The initial rate method (*28*, *29*) was applied in order to determine the ratio of phototransformation quantum efficiencies and the mole fractions of P_r and P_{fr} in photoequilibrium with 644-nm light. Samples at different pH values were successively prepared from an unbuffered stock solution of phytochrome in 50 mM KCl by adding small aliquots of concentrated Tris-HCl buffer. The pH dependence of the P_r and P_{fr} absorption spectra of Cph1 and Cph1Δ2 is very similar (data are shown only for Cph1Δ2; Figure 2A−F).

As shown in Figure 2A, both the wavelength of maximal absorbance and the extinction coefficient of the longest wavelength absorption band (the Q_y-band) of P_r are pH dependent. The spectra were scaled to an extinction coefficient of 85.000 M^{-1} cm^{-1} (pH 7.8), estimated for these preparations.[2] The pH difference spectra (Figure 2C) showed, with increasing pH, a decrease of the absorption of the Q_y-band, whereas blue-shifted bands appeared at 550 and 340 nm. Since similar spectral changes were observed in the pH titrations of the model compounds biliverdin dimethyl ester (*38*) and octaethylbiliverdin (*39*), these changes are most likely due to the formation of the deprotonated species of P_r. At high pH, the absorption maximum of the Q_y-band of both Cph1 and Cph1Δ2 blue shifted to a very similar extent. At pH 6.6, $\lambda_{max}(P_r) = 658.7$ nm, whereas at pH 9.0 $\lambda_{max}(P_r) = 653.7$ nm in the case of Cph1Δ2. Figure 2E shows that the shapes of the titration curves are complex and depend strongly on the wavelength. An analysis with a single Henderson−Hasselbalch curve is thus not possible. Instead, a model was applied that assumes independent deprotonation of two titratable groups, the chromophore (X) and an unknown amino acid side chain (Y). Using this model and assuming full depletion of the Q_y-band at high pH (i.e., when X is deprotonated), the pH dependence of the absorption was fitted simultaneously at nine wavelengths (from 638 to 682 nm in steps of 5.5 nm). The fit yielded approximate values for the two pK_a's of Cph1Δ2: $pK_Y = 7.55 \pm 0.05$ and $pK_X = 9.75 \pm 0.10$ (for experimental data and fitted curves (−) at 638, 660, and 671 nm, see Figure 2E). The spectrophotometric titrations of the model compounds biliverdin dimethyl ester (*38*) and octaethylbiliverdin (*39*) showed, however, that the residual absorbance of the deprotonated form in the Q_y-band is not quite zero but is actually about 30% of that of the protonated form. We therefore explored the effect of a nonzero absorbance of the deprotonated form

[2] Lamparter, Esteban, and Hughes. Personal communication.

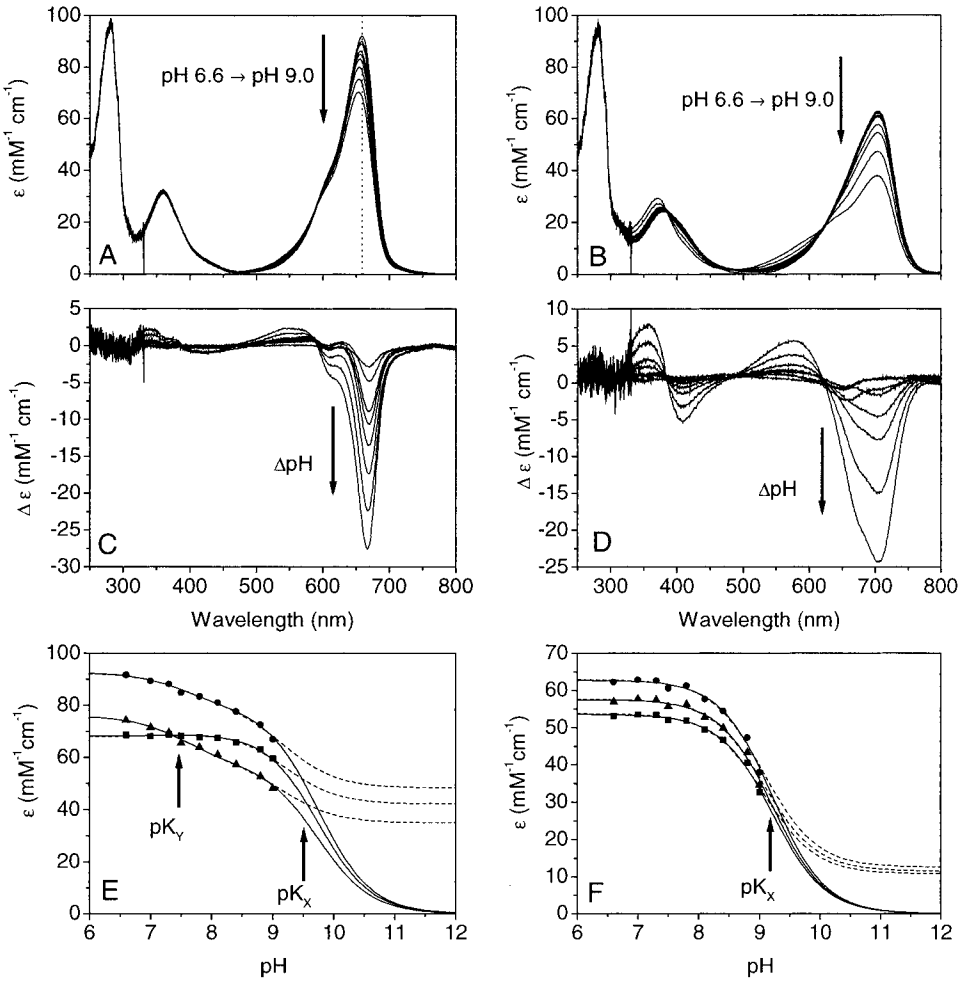

FIGURE 2: pH dependence of the absorption spectra of P_r and P_{fr}. The absorption spectra were scaled to $\epsilon_{658\,nm} = 85.000\ M^{-1}\ cm^{-1}$ at pH 7.8 (see Results). Spectra for Cph1Δ2 are presented because of the minimal light scattering of these samples but are also representative for the results obtained with Cph1. (A) pH dependence of Cph1Δ2 absorption spectra in the P_r state. Spectra are plotted for pH 6.6, 7.0, 7.3, 7.5, 7.8, 8.1, 8.4, 8.8, and 9.0. A dotted vertical line is drawn through the absorption maximum of the Q_y-band at pH 6.6 to highlight the blue shift at higher pH values. (B) Calculated P_{fr} absorption spectra of Cph1Δ2 plotted for pH 6.6−9.0 (see panel A). (C) pH difference spectra for P_r. Changes in extinction coefficient are plotted for the pH values 7.0, 7.3, 7.5, 7.8, 8.1, 8.4, 8.8, and 9.0 after subtraction of the pH 6.6 spectrum. (D) pH difference spectra for P_{fr} (see panel C). (E) pH dependence of the absorption at three selected wavelengths for the P_r state of Cph1Δ2: 638 (■), 660 (●), and 671 nm (▲). The data at nine wavelengths were fitted simultaneously to a model (solid lines) involving independent deprotonation of two titratable groups, X and Y, and assuming that only the species (XH,YH) and (XH,Y^-) contribute to absorption. Alternatively, the data were fitted allowing a residual absorption for X^- of 60% of that of the species (XH,Y^-) (dashed lines). The approximate pK_a's are indicated by arrows. (F) pH dependence of the absorption at three selected wavelengths for the P_{fr} state of Cph1Δ2: 682 (■), 704 (●), and 715 nm (▲). The data at nine wavelengths were fitted simultaneously to the Henderson−Hasselbalch equation (solid lines) and to a model assuming a residual absorption for the deprotonated species of 20% (dashed lines).

on the analysis and fit of the titration data. When the assumption of zero absorbance of the species with deprotonated chromophore (X^-) is relaxed, pK_X shifts to a slightly lower value, while pK_Y is almost unaffected. The quality of the fit, as measured by the χ^2 value, deteriorates only moderately with an increasing extinction coefficient of X^-. Setting the upper limit for a still acceptable value of χ^2 at 1.3× the minimal value, we obtained a conservative estimate of pK_X and its error: p$K_X = 9.5 \pm 0.3$. A residual absorption for X^- of 60% of that of the protonated form (XH, Y^-) still led to a satisfactory fit with a χ^2 below this upper limit. The corresponding fitted curves are shown in Figure 2E (- - -). The data for Cph1 showed a qualitatively similar pH dependence but did not allow determination of the pK_a's with comparable accuracy. Unfortunately, the titrations could only be carried out between pH 6.5 and pH 9.0 due to aggregation and denaturation, particularly of Cph1.

The P_{fr} spectra were obtained from the absorption spectra in photoequilibrium with 644-nm illumination, using the photoconversion rate analysis (Table 1) for calculation of the mole fractions of P_r and P_{fr} in equilibrium. In contrast to the P_r spectra, the calculated P_{fr} spectra showed no pH dependence of the absorption maximum of the Q_y-band (λ_{max}-(P_{fr}) = 703.8 nm) but displayed a decrease of the extinction coefficient for high pH values, as for the P_r spectra (Figure 2B). On the basis of the similarities with the difference spectra of the chromophore model compounds (*38*, *39*), the appearance of blue-shifted species (at 580 and 360 nm) and of negative bands around 410 and 704 nm again most likely reflects formation of a deprotonated form of P_{fr} (Figure 2D). The absence of a blue shift in the Q_y-band and approximate isosbestic points in the P_{fr} difference spectra (Figure 2D) justifies a two-state analysis of the titration data. Assuming again that the extinction coefficient of P_{fr} is zero at high

Table 1: pH Dependence of Phototransformation Quantum Yield Ratios and $P_r \rightarrow P_{fr}$ Photoequilibrium for Cph1 and Cph1Δ2[a]

sample	pH	ϕ_R/ϕ_{FR}	mole fraction P_{fr} in photoequilibrium
Cph1	7.0	1.15	0.71
	7.5	1.15	0.71
	8.1	1.07	0.70
	8.4	1.19	0.72
	8.8	1.02	0.71
	9.0	1.15	0.72
Cph1Δ2	6.6	1.13	0.69
	7.0	1.02	0.68
	7.3	1.05	0.69
	7.5	1.09	0.69
	7.8	1.00	0.68
	8.1	1.10	0.69
	8.4	1.05	0.69
	8.8	1.05	0.69
	9.0	1.05	0.70

[a] The phototransformation rates of Cph1 and Cph1Δ2 were obtained under conditions of red (644 nm) and far-red (735 nm) light illumination. Initial rate analysis (see Materials and Methods) was applied in order to calculate the mole fraction of P_{fr} in photoequilibrium with 644-nm illumination and the phototransformation quantum yield ratio.

pH, simultaneous fitting of the absorption spectra at nine wavelengths (from 682 to 726 nm) to the Henderson−Hasselbalch equation yielded approximate values for the pK_a value of P_{fr}. For Cph1, p$K_a(P_{fr}) = 9.4 \pm 0.2$ was found, and for Cph1Δ2, p$K_a(P_{fr}) = 9.2 \pm 0.1$ (Figure 2F). The data and the fits at three selected wavelengths are shown in Figure 2F. If the deprotonated form of P_{fr} were to show residual absorbance, the pK would shift to a lower value as for pK_X in the case of P_r. A satisfactory fit could still be obtained up to a residual absorbance of 20% and is shown in Figure 2F (- - -). Since the shift of the pK exceeds only slightly the indicated error from the fit with the Henderson−Hasselbalch equation, the pK from that analysis provides a good estimate. In view of the associated uncertainty ranges, the pKs for deprotonation of the chromophore may be considered to be equal in P_r and P_{fr}.

The analysis of phototransformation rates showed that, for both Cph1 and Cph1Δ2, the photoequilibrium attained upon excitation with 644-nm light was hardly affected by pH, in the range of 6.6−9.0 (Table 1). It was found that during the time scale of the experiments, the absorption spectrum in photoequilibrium did not change upon switching off the 644-nm illumination, which shows that excitation of long-living intermediate states by the measuring beam of the spectrophotometer did not contribute to the overall phototransformation efficiencies. In addition, analysis of the transient absorption changes at 720 nm and at pH 7.0 showed that the photoconversion with red and far-red light, respectively, could be satisfactorily fitted with a single exponential rate constant, indicating that both transitions show essentially first-order overall kinetics (Figure 3). In the whole pH range investigated (6.6−9.0), the phototransformation kinetics could be described by a single exponential component (data not shown). The phototransformation analysis, based on Butler's equations (see Materials and Methods and also refs *28* and *29*), is therefore a valid approach for determining the mole fraction of P_{fr} present in photoequilibrium with 644-nm excitation, $x_{P_{fr}}^{644}$. For a sample of Cph1 at pH 7.0, the absolute value for ϕ_R was estimated to be approximately 0.14,

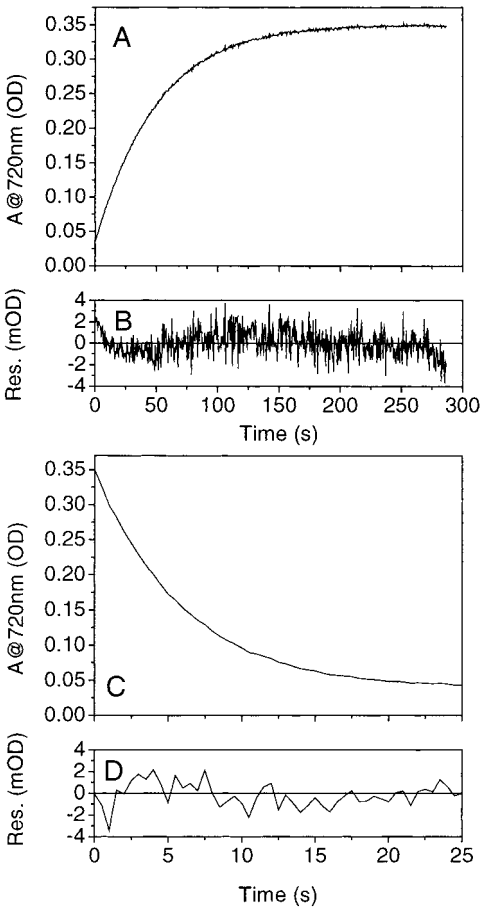

FIGURE 3: $P_r \rightarrow P_{fr}$ and $P_{fr} \rightarrow P_r$ phototransformation characteristics of Cph1. Typical $P_r \rightarrow P_{fr}$ and $P_{fr} \rightarrow P_r$ phototransformation kinetics of Cph1 at pH 7.0. (A) Absorption change at 720 nm with 644-nm illumination, starting in the pure P_r state. The data were fitted with a single exponential with a time constant $\tau = 49.11 \pm 0.08$ s. (B) Residuals for the fit to the data presented in panel A. (C) Absorption change at 720 nm with 735-nm illumination, starting in the P_r/P_{fr} photoequilibrium. The data were fitted with a single exponential with time constant $\tau = 5.96 \pm 0.02$ s. (D) Residuals for the fit to the data presented in panel C.

in resonable agreement with the results of 0.16 from an earlier study (*5*).

Flash-Photolysis Experiments. To find out whether the kinetics of proton release and uptake are directly coupled with the kinetics of the photocycle, transient absorbance measurements were carried out under exactly the same conditions as the transient pH indicator experiments. If the deprotonation reactions are coupled to particular transitions between intermediates, then the corresponding rate constants and amplitudes may be pH dependent. It was thus important to test the pH dependence of the photocycle kinetics. Finally, no photocycle data were available for the N-terminal chromophore carrying domain Cph1Δ2. We therefore investigated the photocycles of Cph1 and Cph1Δ2 at pH 7 and pH 8. Transient absorption data were collected without background illumination at 22−27 wavelengths from 550 to 750 nm for samples of Cph1 at pH 7.0 and pH 8.1−7.9. For Cph1Δ2, data were collected only at the three wavelengths 655, 675, and 705 nm. Typical transient absorption data for Cph1Δ2 are shown in Figure 4A. SVD analysis for the Cph1 data revealed three relevant spectral components. Additional components, with singular values of less than 2%,

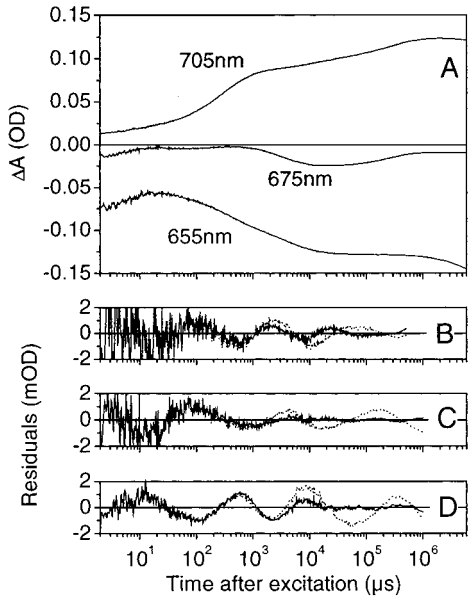

FIGURE 4: Typical transient absorbance changes $\Delta A(t)$ at three diagnostic wavelengths for Cph1Δ2 at pH 7.0 and residuals of exponential fits to the data**.** (A) Time traces at 705, 655, and 675 nm. Optical path length, 1 cm. (B−D) Residuals of a simultaneous fit to the data at the three wavelengths: (B) 655, (C) 675, and (D) 705 nm. The solid lines represent the residuals for a fit with five exponentials (5.2 and 280 μs and 3.5, 21, and 270 ms), while the dotted lines are the residuals for the fit with four exponentials (5.3 and 280 μs and 4.3 and 210 ms). The fit with five exponentials is significantly better in the slower time domain, especially for the data at 705 nm.

were neglected. The time traces of the first three singular components were fitted simultaneously in the time range from 2 μs to 500 ms with a sum of five exponentials (τ_1−τ_5). The analysis was limited to a 500-ms time window because for wavelengths close to λ_{max} of P_r the measuring light contributed to the $P_r \rightarrow P_{fr}$ transition in the slowest time domain (>500 ms). As a consequence, the slowest time constant, τ_5 (~300 ms), was less accurately determined than the time constants of the faster components. Global analysis of the Cph1 data collected at 22−27 wavelengths indicated five relevant rate constants at both pH values (Table 2). Simultaneous fitting of the Cph1Δ2 data, collected at only three wavelengths, also indicated that five time constants are required for an adequate fit. Figure 4B−D shows the significant reduction in the fit residuals when the number of exponentials was increased from four to five. The amplitude spectra calculated from the SVD basis spectra and from the amplitudes of the fits of the SVD time traces for Cph1 at pH 7 and pH 8 are shown in Figure 5.

Comparison of lines one and two or lines three and four of Table 2 shows that an analysis based on the Cph1 data at only three wavelengths (655, 675, and 705 nm) led to time constants that were, within experimental error, identical to those obtained by global analysis based on measurements at 22 or 27 wavelengths. This justified the use of these three wavelengths only for the measurements with Cph1Δ2. The results of the photocycle kinetics for Cph1 and Cph1Δ2 at pH 7 and pH 8 are summarized in Table 2. The time constants for Cph1Δ2 are very similar to those for Cph1. The same holds for the amplitudes. We conclude that the transmitter module that is missing in Cph1Δ2 has a negligible effect on the photocycle kinetics. From Table 2, we can also conclude that the pH dependence of the time constants, at least in the range from pH 7 to pH 8, is very small.

Significant differences were observed when the amplitude spectra for the Cph1 samples at pH 7.0 and pH 8.1−7.9 were compared (Figure 5). The amplitude of the ~5 μs component τ_1 is larger at pH 7.0 at 655 nm, whereas the feature at 705 nm is smaller. The amplitude spectrum of the ~4-ms component is changed as well, particularly in the 700−750-nm region. The amplitude of the slowest component, τ_5, increased at pH 8. The calculated final difference spectra for the measurements performed without continuous far-red light illumination (B_0 in Figure 5) should be proportional to the $P_{fr}-P_r$ difference spectrum. Small deviations between these scaled spectra were only observed in the 600−680-nm region, indicating some contribution of the measuring beam to the $P_r \rightarrow P_{fr}$ transition in the time domain of seconds (not shown). For the wavelengths above 680 nm, an excellent agreement was found between the final extrapolated spectrum and the $P_{fr}-P_r$ difference spectrum, allowing calculation of the efficiency of excitation (η, Table 3). Fitting of the transient absorption traces collected with continuous background illumination required addition of one rate constant, reflecting reformation of P_r. The required additional time constant was 750 ms for irradiation with the highest intensity of far-red background light.

Proton Release and Uptake during the $P_r \rightarrow P_{fr}$ Transition. Samples of Cph1 and Cph1Δ2 were prepared without pH buffer at $OD_{660} \sim 1.5$, with 13 μM fluorescein included as a pH indicator. Difference absorption traces were obtained at 655, 675, and 705 nm to determine the photocycle kinetics and η for these samples. From the analysis of these transients, it was determined that the photocycle time constants were not significantly affected by the addition of the pH indicator dye (compare the even and odd rows in Table 2). As shown in Figure 6, transients at 490 nm (the λ_{max} of the deprotonated dye) were recorded for samples with identical phytochrome concentration and pH with (F+) and without (F−) fluorescein. Subtraction of these transients yielded the flash-induced time-resolved changes of absorption of fluorescein $\Delta\Delta A$ (Figure 6). As shown in the inset of Figure 6A, the wavelength dependence of the release-phase amplitude was proportional to the pH-induced difference spectrum of fluorescein, indicating that this transient was due to the protonation of the dye. An initial proton release phase was detected in the millisecond time domain followed by proton uptake in about 300 ms. The amplitude of the proton uptake component was smaller than the amplitude for the release component, resulting in a net acidification of Cph1 and Cph1Δ2 in the P_{fr} form. This can be clearly seen in Figure 6A, without continuous far-red background illumination, where the $\Delta\Delta A_{490}$ transient does not return to the baseline for long times, reflecting a difference in the degree of protonation between the initial P_r state and the final P_{fr} state. Judging from this $\Delta\Delta A_{490}$ trace, it appears that first (minimum around 50 ms) about twice as many protons are released as are ultimately (plateau around 4 s) released in P_{fr}. When the transients at 490 nm were collected under conditions of continuous far-red illumination, the $\Delta\Delta A_{490}$ transient did return to the baseline after several seconds due to the complete reformation of P_r (Figure 6B). The net acidification observed in the transient pH indicator experiments in the second time range in the absence of far-red background

Table 2: Photocycle Kinetics of Cph1 and Cph1Δ2 at pH 7.0 and pH 8[a]

sample	pH	fluorescein (μM)	analysis/λ (nm)	τ_1 (μs)	τ_2 (μs)	τ_3 (ms)	τ_4 (ms)	τ_5 (ms)
Cph1	7.0	0	global	4.9	320	4.2	24	200
Cph1	7.0	13	655, 675, 705	4.6	310	3.9	32	230
Cph1	8.1−7.7	0	global	4.5	270	3.8	30	280
Cph1	8.1−7.9	13	655, 675, 705	4.2	230	3.2	44	410
Cph1Δ2	7.0	0	655, 675, 705	5.2	280	3.5	21	270
Cph1Δ2	7.0	13	655, 675, 705	5.1	290	3.4	18	270
Cph1Δ2	8.3−7.7	0	655, 675, 705	4.9	190	2.4	36	460
Cph1Δ2	8.3−7.7	13	655, 675, 705	4.6	210	2.9	33	320

[a] Flash photolysis was performed with samples of Cph1 and Cph1Δ2 at pH 7.0 and pH ~8.0. The drift in pH was due to the absence of pH buffer. Samples with or without fluorescein present as a pH indicator were analyzed for determination of the phototransformation kinetics. Global analysis here implies that absorption changes were measured at 22−27 wavelengths between 545 and 755 nm, that the data were reduced by SVD, and that the traces of the relevant SVD components were fitted simultaneously.

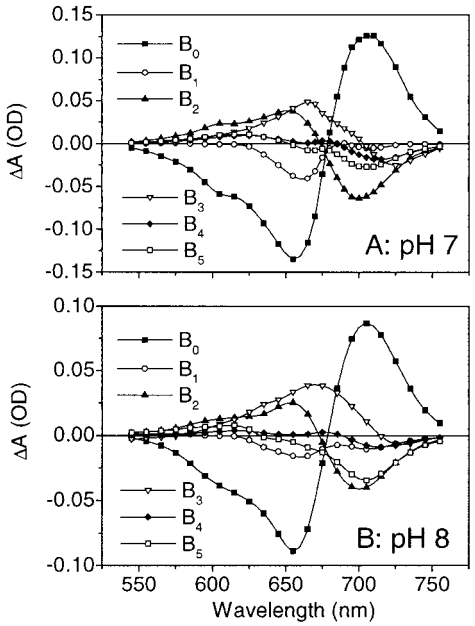

FIGURE 5: Lifetime-associated amplitude spectra of Cph1 at pH 7 and pH 8. The amplitude spectra B_1-B_5 were calculated from transient absorption measurements without continuous background illumination performed with Cph1 at pH 7.0 (A) and pH 8.1−7.9 (B), as detailed in Materials and Methods. The related time constants are $\tau_1 = 4.9$ μs, $\tau_2 = 320$ μs, $\tau_3 = 4.2$ ms, $\tau_4 = 24$ ms, and $\tau_5 = 200$ ms for pH 7 (A) and $\tau_1 = 4.5$ μs, $\tau_2 = 270$ μs, $\tau_3 = 3.8$ ms, $\tau_4 = 30$ ms, and $\tau_5 = 280$ ms for pH 8 (B). A positive amplitude signifies a decay component, whereas a negative amplitude signifies a rise term. B_0 is the difference spectrum between the initial and the final state and should correspond to the difference between P_r and P_{fr}.

illumination (Figure 6A) is in good agreement with the results of the steady-state pH-electrode measurements.

The $\Delta\Delta A_{490}$ traces reflecting transient bleaching of fluorescein, due to transient proton uptake by the indicator dye, could be fitted reasonably well with the time constants $\tau_3-\tau_5$ derived from the photocycle measurements of the same samples (Figure 6). In the example shown (Figure 6; Cph1Δ2, pH 7.0), however, a better fit was achieved when the value of the τ_4 component in the transient absorption signal (Table 2) was decreased from 18 to 12.4 ms (dashed line in Figure 6). This was justified, since the small amplitude of τ_4 in the photocycle (see Figure 5; B_4) led to a relatively large error in its time constant. It was therefore concluded that the kinetics of proton release and uptake were described, within experimental accuracy, by the photocycle time constants $\tau_3-\tau_5$. In measurements with continuous background illumination with far-red light, these same time constants could be used for fitting the traces in addition to a single 750-ms component with negative amplitude, reflecting reformation of P_r (Figure 6B).

The number of transient protons released per $P_r \rightarrow P_{fr}$ transition, calculated using titration with oxalic acid, equals approximately one for both Cph1 and Cph1Δ2 at pH 7 and pH 8 (Table 3, column $H^+/P_r \rightarrow P_{fr}$ (max)). For both proteins, the net acidification in P_{fr} is higher at the lower pH (Table 3, last column), in agreement with the pH-electrode results.

DISCUSSION

pH Dependence of the P_r and P_{fr} Absorption Spectra. The absorption spectra of both P_r and P_{fr} are pH dependent. The absorption maximum of the S_0-S_1 transition blue shifts at high pH only in the case of P_r. Thus, there must be a difference between P_r and P_{fr} with respect to electronic interactions between a protonatable side chain ($pK_Y = 7.55 \pm 0.05$) and the chromophore. In view of the tentative p*K*, this transition might reflect protonation of a histidine residue adjacent to the chromophore (*4*, *5*). Addition of imidazole, which is chemically identical to the histidine side chain, also results in a blue shift of the P_r absorption maximum from 655 to 648 nm at pH 7.8 (*9*). The present results imply that imidazole in its deprotonated form interacts directly with the chromophore, which results in the observed spectral changes.

In addition, both species show a decrease of absorbance in the Q_y-band with increasing pH. The formation of a deprotonated species is observed in the difference spectra of both P_r and P_{fr}. In the case of P_r, troughs at 425 and 655−660 nm and peaks at 340 and 550 nm are present in the pH difference spectra, indicative of the formation of a deprotonated linear tetrapyrrole (*38*−*40*). Likewise, in the P_{fr} spectra, troughs at 410 and 704 nm and peaks at 360 and 580 nm are present (Figure 2C,D). The pH-induced difference absorbance is more pronounced for P_{fr} than for P_r, in particular in the Soret region, and the amplitudes of the positive difference bands as compared to the negative bands are larger than in P_r (Figure 2A,C). Qualitatively, these pH difference spectra (Figure 2C,D) resemble the pH difference spectra for the model compounds biliverdin dimethyl ester (*38*) and octaethylbiliverdin (*39*). The similarities include the typical pattern of four alternatingly positive and negative bands and the very large difference in the Q_y-band. Our conclusion that the chromophore is protonated in both P_r and

Table 3: Kinetics and Quantification of the Transient Proton Release and Proton Uptake Phases[a]

		photocycle kinetics			fluorescein transient signal (at 490 nm)			
sample	pH	$OD_{655\ nm}$	η (%)	τ_3, τ_4, τ_5 (ms)	ΔA_{max} mOD	$H^+/P_r \rightarrow P_{fr}$ (max)	ΔA_{stable} mOD	$H^+/P_r \rightarrow P_{fr}$ (stable)
Cph1	7.0	1.75	9.5 ± 0.5	3.9, 32, 230	−0.8	1.0 ± 0.4	−0.6	0.8 ± 0.3
Cph1	8.1−7.9	0.95	13.5 ± 1.0	3.2, 44, 410	−0.45	1.0 ± 0.3	−0.2	0.5 ± 0.2
Cph1Δ2	7.0	1.55	9.5 ± 0.5	3.4, 18, 270	−2.8	1.2 ± 0.3	−1.3	0.5 ± 0.2
Cph1Δ2	8.3−7.7	1.30	9.5 ± 0.5	2.9, 33, 320	−1.3	0.9 ± 0.4	−0.4	0.3 ± 0.2

[a] Unbuffered samples of Cph1 and Cph1Δ2 with fluorescein included as a pH indicator dye were analyzed for transient absorption changes at 490 nm due to transient protonation of the dye. The excitation efficiency, η, was calculated as described in the Results. The $H^+/P_r \rightarrow P_{fr}$ stoichiometry was calculated from the absorbance change of fluorescein using a microacid titration. The experimental values are given with estimated errors. ΔA_{max} and ΔA_{stable} are the maximal transient dye absorbance change (after ~50 ms) and its final value, respectively (see Figure 6A). Corresponding to these values, the stoichiometries of proton release, $H^+/P_r \rightarrow P_{fr}$ (max) and $H^+/P_r \rightarrow P_{fr}$ (stable), were calculated from acid-shot calibrations. mOD: milli.OD.

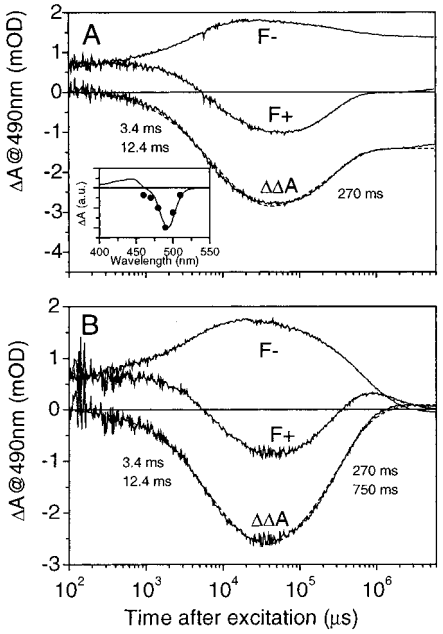

FIGURE 6: Kinetics of flash-induced proton release and uptake during the $P_r \rightarrow P_{fr}$ transition. Typical proton release and proton uptake measurements with Cph1Δ2 at pH 7.0. Difference absorption transients at 490 nm were recorded of samples of Cph1Δ2 with (F+) and without (F−) fluorescein at pH 7.0. The transient absorption decrease $\Delta\Delta A$ at 490 nm, due to proton release of Cph1Δ2 and detected by the protonation of fluorescein, was obtained by subtraction of the F+ and F− traces. (A) Absorption transients without continuous far-red background light. The trace was averaged from 30 flash measurements with a sample that was returned to the initial state (pure P_r) between measurements by preillumination with far-red light. A fit (dashed trace) is shown, using two time constants for the proton release phase and one constant for the proton uptake phase. The inset shows that the wavelength dependence for the $\Delta\Delta A$ amplitude (●) follows the scaled difference spectrum for the $pK_a = 6.4$ transition of fluorescein (−). The end value of $\Delta\Delta A$ at 5 s corresponds to ΔA_{stable} of Table 3. The maximal value of $\Delta\Delta A$ around 50 ms corresponds to ΔA_{max} of Table 3. (B) Absorption transients with continuous far-red background light, averaged from 30 measurements. The fit shown (dashed trace) was made by including an additional 750-ms time constant, reflecting P_r reformation due to the far-red background light.

P_{fr} at physiological pH is mainly based on this striking similarity with the titration data for the chromophore model compounds and is in agreement with recent proposals based on FTIR spectroscopy of Cph1 (*11*). Taking the residual absorbance of the species with deprotonated chromophore in the Q_y-band into account, we obtained similar values of 9.5 ± 0.3 and 9.2 ± 0.1 for pK_X in the P_r and the P_{fr} forms of Cph1, respectively. So, within experimental error, the pK_a's are equal. This is consistent with our observation that the P_r/P_{fr} ratio at photoequilibrium is independent of pH up to at least pH 9 (Table 1).

Our pH titration experiments indicated that at alkaline pH the chromophores of P_r and P_{fr} deprotonate. So, at high pH, there are also species present with deprotonated chromophores, designated P_r^- and P_{fr}^-. Our initial rate analysis of the photoequilibrium data was based however on the assumption of a two-state equilibrium between P_r and P_{fr}. This assumption is justified by and consistent with the results of our spectral titrations, which led to equal pK_a's for the chromophore deprotonation in P_r and P_{fr}. Under those conditions, the photoequilibrium is decoupled from the chromophore deprotonation equilibria and is not affected by the latter. The model-compound spectra showed moreover that the absorbance in the Q_y-band of the deprotonated species is only about 30% of the protonated form (*38*, *39*). Assuming this also to be true for the P_r and P_{fr} forms of Cph1, we conclude that the species with deprotonated chromophore can only be weakly excited in the photoequilibrium experiments and therefore do not contribute substantially in the photoequilibrium. Finally, only a single exponential component was detected in the phototransformation kinetics, even at pH 9. Thus, also experimentally, there is no evidence for heterogeneity due, for example, to different phototransformation kinetics for $P_r \rightarrow P_{fr}$ and $P_r^- \rightarrow P_{fr}^-$.

Because the analysis indicates that two separate pKs have to be distinguished in the titration of P_r, we propose that the blue shift of the S_0-S_1 transition of the latter reflects deprotonation of an unidentified amino acid side chain, possibly a histidine, whereas the decrease in absorption is due to deprotonation of the chromophore itself. Significantly, under our experimental conditions, the absence of the histidine kinase domain in Cph1Δ2 neither affects the spectral properties of P_r and P_{fr} nor affects the phototransformation efficiency for either the $P_r \rightarrow P_{fr}$ or the $P_{fr} \rightarrow P_r$ transition.

Flash Photolysis. In the previously published flash photolysis work (*10*), data were only reported for Cph1 and under quite restricted conditions (one pH value, 50 mM Tris, 10 °C). Extensive photocycle measurements were therefore required to (1) investigate the pH dependence of the cycle; (2) investigate the cycle for the sensory module Cph1Δ2; (3) assign the proton uptake and release steps to particular

transitions in the photocycle, which required data under precisely the same conditions as for the transient dye experiments (22 °C, 50 mM KCl, pH close to the p*K* of the dye); and (4) check for possible effects of the pH indicator dye on the photocycle kinetics.

High-quality data for Cph1 were collected over a broad wavelength range (550−750 nm) and with a logarithmic time base covering the entire time range from 50 ns to seconds in a single shot. The transient absorption measurements were performed for Cph1 and Cph1Δ2 at pH 7.0 and pH 8.0. For Cph1 at pH 8.0, our results are in accord with the main conclusions of Remberg et al. (*10*). In particular, we confirm the existence of the novel intermediate with a rise time of ∼300 μs (τ_2) and a decay of ∼3 ms (τ_3) (*10*) that is not detected in the phototransformation of higher plant phytochromes (*8*). This intermediate is of great interest for our work on the proton release, since its formation and decay exhibit a large deuterium kinetic isotope effect (*10*). For Cph1Δ2, we now report the occurrence of an intermediate with very similar kinetics (Table 2).

The amplitude of the fastest component detected in our measurements was negative with a time constant of about 5 μs (Figure 5; B_1), whereas Remberg et al. (*10*) reported a fastest time constant of 25 μs with a positive amplitude. We have no explanation for this discrepancy, but we note that it does not affect our arguments on proton release since that occurs on a much slower time scale. Another minor difference with ref *10* is that in our data analysis we did not need a biexponential fit to describe the P_{fr} formation. Instead, we needed an additional component with a time constant of about 30 ms (τ_4) with a similar amplitude spectrum as the term τ_5 that reflects P_{fr} formation (Figure 5A,B; B_4 component).

The five time constants $\tau_1-\tau_5$, collected in Table 2, show that the kinetics of the photocycle of Cph1 and Cph1Δ2, its N-terminal chromophore carrying domain, are quite similar. This is not very surprising since the electronic transitions of the chromophore are not expected to be sensitive to molecular events in the remote transmitter module. Table 2 also shows that changing the pH from 7 to 8 only leads to minor changes in the time constants. Taking the errors into account, these trends were not considered to be significant. More pronounced pH effects were detected in the amplitude spectra of the components described by τ_1, τ_3, and in particular τ_5 (B_5 component in Figure 5). Significant deuterium kinetic isotope effects have been reported for the rise (τ_2) and decay (τ_3) of the novel intermediate that is unique to Cph1 (*10*). It is therefore of particular interest that, in addition to displaying this isotope effect, τ_3 also has a pH-dependent amplitude spectrum and is associated with proton release. It is puzzling on the other hand that τ_2, which is also reported to show a kinetic isotope effect, does not have a pH-dependent amplitude spectrum and is not coupled to the release or uptake of protons.

Proton Release and Uptake during the $P_r \rightarrow P_{fr}$ Transition. The results of the pH titration of the P_r and P_{fr} spectra imply that there is no difference in the degree of protonation of the chromophore between these states at physiological pH. This interpretation of our titration data is supported by recent FTIR experiments with Cph1 at pH 7.8 from which it was concluded that the chromophore is protonated in both P_r and P_{fr} (*11*). The proton release leading to the net acidification in P_{fr} must thus originate from titratable groups of amino acid side chains of Cph1. The titration experiments do not exclude the possibility of transient chromophore deprotonation and reprotonation between P_r and P_{fr}, but the results from vibrational spectroscopy (*11*) showed that at least in the meta-R_a intermediate at pH 7.8 the chromophore was still protonated. We will therefore assume that the chromophore remains protonated throughout the photocycle. This implies that all the transient protonation changes are due to pK_a changes in the protein moiety. These pK_a shifts might be due to electronic reconfiguration of one or more solvent-exposed groups or to transient exposure of one or more protonatable groups to the solvent. We cannot discriminate between these possibilities.

The proton release phase could be well-described by the photocycle time constants τ_3 (∼3 ms) and τ_4 (∼12 ms). The proton release is thus associated at least in part with the decay of the novel intermediate (τ_3) that has the large deuterium isotope effect. The uptake phase was coupled to the rise of P_{fr} with τ_5 (∼270 ms). In this way, we have time resolved the structural transitions that cause the pK_a shifts. The time-resolved proton signal serves here as a sensitive monitor for conformational changes.

The amplitude of the proton uptake phase was smaller than that of the release phase leading to net acidification in P_{fr} for both Cph1 and Cph1Δ2 (see Figure 6A and last column in Table 3). This is in good agreement with the pH-electrode measurements. This net acidification observed in the transient proton release and uptake measurements was significantly larger at pH 7 than at pH 8 for both Cph1 and Cph1Δ2 (last column in Table 3). These observations are also in good agreement with the pH-electrode data, which covered a wider pH range. The question arises why the net proton release is larger at lower pH. Because the number of transiently released protons is within experimental error, independent of pH (Table 3, column 7), the effect must be due to a decrease in the amplitude of the proton uptake phase with decreasing pH. This can be formally described as an inhibition of the extent of the uptake phase (τ_5) by an increase in the external proton concentration. Because τ_5 is virtually pH independent (Table 2), this effect is most likely simply due to a pK_a shift of the appropriate sign and magnitude in the formation of P_{fr} (τ_5).

The amplitude spectra for τ_4 and τ_5 are very similar, in particular for the sample at pH 7.0 (Figure 5A; B_4 and B_5). Both phases might contribute to P_{fr} formation, particularly when parallel pathways are considered; however, it should be noted that the amplitudes for the proton release kinetics are opposite for τ_4 and τ_5. This indicates that dissimilar conformational changes are associated with these transitions, making a parallel pathway less likely.

Under the conditions selected, the rate of protonation of fluorescein was limited by the rate of the underlying conformational change in Cph1 and/or Cph1Δ2. The second-order rate constant for protonation of fluorescein is 2.0×10^{10} M^{-1} s^{-1}, allowing detection of proton release in the microsecond time domain (*18*, *41*). Because of the buffering strength of samples containing protein, the observed time constants for protonation of such dyes are typically ∼65−500 μs, as shown with studies of proton release by bacteriorhodopsin (*18*, *31*, *42*, *43*). The fastest component for fluorescein protonation in our experiments was 3−4 ms,

indicating that diffusion was not limiting. In addition, control experiments with pyranine as the pH indicator did not result in an apparent acceleration of the proton release phase, even though the second-order rate constant for protonation of pyranine is significantly higher than for fluorescein (i.e., 1.8×10^{11} M^{-1} s^{-1}; *41*).

Light-Induced Reversible Acidification of Unbuffered Phytochrome Solutions. Simultaneous recording of the absorption changes and the pH changes during red and far-red irradiation of unbuffered phytochrome solutions allowed determination of the $H^+/P_r \rightarrow P_{fr}$ stoichiometry for a larger range of pH values than was covered in the transient pH indicator experiments. The latter measurements are limited to a narrow pH range around the p*K* of the dye. In agreement with the dye experiments, it was found that stable acidification in the P_{fr} state increased with decreasing pH, in the case of both Cph1 and Cph1Δ2 (Figure 1B). The $H^+/P_r \rightarrow P_{fr}$ stoichiometry of this stable acidification was however smaller than when quantified by the flash-photolysis approach (Table 3).

The pH-electrode measurements required a 1 M KCl concentration for an optimal signal/noise ratio of the electrode (*37*), necessitating minor corrections for increased light scattering resulting from limited phytochrome precipitation. The flash-photolysis experiments, on the other hand, were performed at low salt concentration (50 mM KCl), where aggregation is negligible. Presumably, the higher salt concentration employed in the pH-electrode measurements stimulates the proton uptake reaction by affecting the p*K* change responsible for the uptake. It is well-known that electrostatic screening in high salt leads to p*K* shifts. A dependence of the extent of light-dependent proton release on the salt concentration has earlier been demonstrated for bacteriorhodopsin (*37*).

Comparison with Proton Release and Uptake in Pea Phytochrome. It is of interest to compare our results on prokaryotic Cph1 with the previous work on eukaryotic pea phytochrome and its fragments (*20*, *21*, *23*). With the 114-kDa fragment and using pH electrodes, these authors observed light-induced alkalization at pH 6.2−7.8, no net proton exchange at pH 7.8, and increasing acidification above pH 7.8. With Cph1, we observed only acidification over the entire accessible pH range from 5.5 to 9.0 (Figure 1B). Moreover, the acidification decreased with increasing pH, approaching zero at pH 9.0. This shape of the pH dependence makes it very unlikely that we would have observed net alkalinization if we had been able to measure below pH 5.5. There thus appears to be a marked difference between the light-induced deprotonation patterns of Cph1 and the 114-kDa fragment from a pea. On the other hand, 121-kDa preparations of pea PhyA showed much lower levels of proton release and uptake (*21*). The authors suggested that in the latter case an N-terminal fragment in the 121-kDa protein blocks the net proton transfer to the aqueous medium. Whether this represents the physiological situation is still unclear, however, because the predicted molecular mass of the native gene product is 124 kDa, similar to that of other plant PhyAs, rather than 121 kDa. There is, however, no doubting that the 121-kDa phytochrome shows an even larger difference with respect to Cph1 than the 114-kDa preparations. Because of the many significant differences between the cyanobacterial and the plant phytochromes (PAS module, unique 3-ms intermediate, histidine kinase activity, P_r active form), it is not surprising that the details of the light-induced protonation changes are different in the two systems, although we note that the effect in Cph1 seems to be independent of the kinase domain. Protonation changes associated with structural changes seem to play an important role in both phytochrome types, however.

In the earlier measurements with pea phytochrome (*21*), no time-resolved data on the kinetics of the transient proton release were reported, and neither could the protonation changes be assigned to particular transitions in the photocycle. On the basis of their later steady-state resonance Raman results (*23*) however, which indicated that the chromophore is protonated in P_r but deprotonated in the I_{bl} intermediate and P_{fr}, these authors suggested that proton release occurs in the formation of I_{bl} and proton uptake occurs in the formation of P_{fr}. In our work with Cph1, we have shown with time-resolved methods that the release indeed precedes uptake and have assigned these reactions to particular transitions in the photocyle. In more recent resonance Raman work with plant phytochrome, it was concluded that the chromophore is protonated in P_r, P_{fr}, and all intermediates (*24*−*26*). The latter results would imply that the argument in ref *23* that the chromophore is the source of the released proton is invalid.

CONCLUSIONS

During the $P_r \rightarrow P_{fr}$ transitions of Cph1 and Cph1Δ2, protons are first released (∼3 ms) and subsequently partially taken up again (∼270 ms). The amplitude of the release component is larger than that of the uptake phase, resulting in net acidification of P_{fr}.

The kinetics of this proton release and uptake were shown to correspond to transitions between particular intermediates in the photocycle of Cph1 and Cph1Δ2. It is concluded that these protonation changes are caused by p*K* changes that are induced by conformational changes of the protein moiety, resulting from chromophore excitation. The identification of the residues involved in proton release and uptake during the photocycle of Cph1 might reveal domains of the protein that are involved in the intramolecular signal transduction from its chromophore-binding domain to its histidine kinase domain.

ACKNOWLEDGMENT

We thank Dr. T. Gensch for stimulating discussions and Ms. B. Esteban for preparing Cph1.

REFERENCES

1. Schaffner, K., Braslavsky, S. E., and Holzwarth, A. R. (1990) *Adv. Photochem. 15*, 229−277.
2. Quail, P. H. (1998) *Philos. Trans. R. Soc. London, Ser. B 353*, 1399−1403.
3. Kaneko, T., Sato, S., Kotani, H., Tanaka, A., Asamizu, E., Nakamura, Y., Miyajima, N., Hirosawa, M., Sugiura, M., Sasamoto, S., Kimura, T., Hosouchi, T., Matsuno, A., Muraki, A., Nakazaki, N., Naruo, K., Okumura, S., Shimpo, S., Takeuchi, C., Wada, T., Watanabe, A., Yamada, M., Yasuda, M., and Tabata, S. (1996) *DNA Res. 3*, 109−136.
4. Hughes, J., Lamparter, T., Mittmann, F., Hartmann, E., Gärtner, W., Wilde, A., and Börner, T. (1997) *Nature 386*, 663.

5. Lamparter, T., Mittmann, F., Gärtner, W., Börner, T., Hartmann, E., and Hughes, J. (1997) *Proc. Natl. Acad. Sci. U.S.A. 94*, 11792−11797.
6. Yeh, K. C., Wu, S. H., Murphy, J. T., and Lagarias, J. C. (1997) *Science 277*, 1505−1508.
7. Hughes, J., and Lamparter, T. (1999) *Plant Physiol. 121*, 1059−1068.
8. Braslavsky, S. E., Gärtner, W., and Schaffner, K. (1997) *Plant, Cell Environ. 20*, 700−706.
9. Hübschmann, T., Börner, T., Hartmann, E., and Lamparter, T. (2001) *Eur. J. Biochem. 268*, 2055−2063.
10. Remberg, A., Lindner, I., Lamparter, T., Hughes, J., Kneip, C., Hildebrandt, P., Braslavsky, S. E., Gärtner, W., and Schaffner, K. (1997) *Biochemistry 36*, 13389−13395.
11. Foerstendorf, H., Lamparter, T., Hughes, J., Gärtner, W., and Siebert, F. (2000) *Photochem. Photobiol. 71*, 655−661.
12. Emeis, D., Kuhn, H., Reichert, J., and Hofmann, K. P. (1982) *FEBS Lett. 143*, 29−34.
13. Parkes, J. H., and Liebman, P. A. (1984) *Biochemistry 23*, 5054−5061.
14. Dickopf, S., Mielke, T., and Heyn, M. P. (1998) *Biochemistry 37*, 16888−16897.
15. Olson, K. D., Deval, P., and Spudich, J. L. (1992) *Photochem. Photobiol. 56*, 1181−1187.
16. Meyer, T. E., Cusanovich, M. A., and Tollin, G. (1993) *Arch. Biochem. Biophys. 306*, 515−517.
17. Hendriks, J., Hoff, W. D., Crielaard, W., and Hellingwerf, K. J. (1999) *J. Biol. Chem. 274*, 17655−17660.
18. Alexiev, U., Mollaaghababa, R., Scherrer, P., Khorana, H. G., and Heyn, M. P. (1995) *Proc. Natl. Acad. Sci. U.S.A. 92*, 372−376.
19. Stryer, L. (1995) *Biochemistry* (4th edition), pp 163−164, W. L. Freeman & Co., New York.
20. Tokutomi, S., Yamamoto, K. T., Miyoshi, Y., and Furuya, M. (1982) *Photochem. Photobiol. 35*, 431−433.
21. Tokutomi, S., Yamamoto, K. T., and Furuya, M. (1988) *Photochem. Photobiol. 47*, 439−445.
22. Furuya, M. (1989) *Adv. Biophys. 25*, 133−167.
23. Mizutani, Y., Tokutomi, S., and Kitagawa, T. (1994) *Biochemistry 33*, 153−158.
24. Kneip, C., Hildebrandt, P., Schlamann, W., Braslavsky, S. E., Mark, F., and Schaffner, K. (1999) *Biochemistry 38*, 15185−15192.
25. Foerstendorf, H., Mummert, E., Schafer, E., Scheer, H., and Siebert, F. (1996) *Biochemistry 35*, 10793−10799.
26. Andel, F., III, Lagarias, J. C., and Mathies, R. A. (1996) *Biochemistry 35*, 15997−16008.
27. Kraayenhof, R., Schuurmans, J. J., Valkier, L. J., Veen, J. P., Van Marum, D., and Jasper, C. G. (1982) *Anal. Biochem. 127*, 93−99.
28. Butler, W. L., Hendricks, S. B., and Siegelman, H. W. (1964) *Photochem. Photobiol. 3*, 521−528.
29. Pratt, L. H. (1975) *Photochem. Photobiol. 27*, 33−36.
30. Otto, H., Marti, T., Holz, M., Mogi, T., Lindau, M., Khorana, H. G., and Heyn, M. P. (1989) *Proc. Natl. Acad. Sci. U.S.A. 86*, 9228−9232.
31. Alexiev, U., Marti, T., Heyn, M. P., Khorana, H. G., and Scherrer, P. (1994) *Biochemistry 33*, 13693−13699.
32. Craven, C. J., Derix, N. M., Hendriks, J., Boelens, R., Hellingwerf, K. J., and Kaptein, R. (2000) *Biochemistry 39*, 14392−14399.
33. Van Thor, J. J., Pierik, A., Nugteren-Roodzant, I., Xie, A., and Hellingwerf, K. J. (1998) *Biochemistry 37*, 16915−16921.
34. Kneen, M., Farinas, J., Li, Y., and Verkman, A. S. (1998) *Biophys. J. 74*, 1591−1599.
35. Arnis, S., and Hofmann, K. P. (1993) *Proc. Natl. Acad. Sci. U.S.A. 90*, 7849−7853.
36. Fahmy, K., Siebert, F., and Sakmar, T. P. (1994) *Biochemistry 33*, 13700−13705.
37. Renthal, R. (1977) *Biochem. Biophys. Res. Commun. 77*, 155−161.
38. Margulies, L., and Stockburger, M. (1979) *J. Am. Chem. Soc. 101*, 743−744.
39. Mizutani, Y., Tokutomi, S., Aoyagi, K., Horitsu, K., and Kitagawa, T. (1991) *Biochemistry 30*, 10693−10700.
40. Krois, D. (1991) *Monatsh. Chem. 122*, 495−506.
41. Gutman, M. (1986) *Methods Enzymol. 127*, 522−538.
42. Drachev, L. A., Kaulen, A. D., and Skulachev, V. P. (1984) *FEBS Lett. 178*, 331−335.
43. Scherrer, P., Alexiev, U., Marti, T., Khorana, H. G., and Heyn, M. P. (1994) *Biochemistry 33*, 13684−13692.

BI002651D